Scintillation Effect on Satellite Communications within Standard Atmosphere

Mohammed Ali Hussein
Electrical Engineering Department, College of Engineering
University of Anbar, Iraq
Tel: 009647901573394
E-mail: elecom1978@yahoo.com

Abstract:
In satellite communications with frequencies above 10GHz the major problems in radio-wave propagation is signal level attenuation caused by tropospheric scintillation, together with signal level attenuation by rain. There are several methods to measure the magnitude of scintillation. The equations of most of these methods do not include meteorological element. In meantime we can not measure the magnitude of scintillation with elevation angle 5˚-10˚. A prediction method is suggested to measure tropospheric scintillation on earth-space path. It would apply this method to standard atmosphere and we studied the effect of meteorological conditions, frequency, antenna diameter and elevation angle on the magnitude of scintillation.

Keywords:
Tropospheric Scintillation, Standard Atmosphere, Fading, Satellite Communication.

1. INTRODUCTION

It is well known that the propagation characteristics of the radio waves are determined by changes in the refractivity of the propagation medium. These changes cause refraction, reflection, guiding or scattering of the waves [1]. They may occur on a time scale of a few minutes (or less) and on longer times scale such as diurnal or seasonal variations. Also small scale variation or irregularities in atmospheric humidity, temperature and pressure which are associated with atmospheric turbulence may cause fluctuation from point-to-point, along the propagation link giving rise to scattering of radio waves [2-3].
The term scintillation, which originated in radio astronomy, is used to describe time variations in channel characteristics due to physical changes in the propagation medium, such as variations in the density of ions in the ionosphere that diffract HF radio waves.
The atmosphere is gaseous layer enveloping the earth and is composed of dry gases and water vapor. It is a mixture of approximately 78% nitrogen, 21% oxygen, and 1% other gases and contains water vapor, which varies in amount from 0 to 5 percent or more. The water vapor exists in significant quantity up to 9km. Troposphere is the lower region of the atmosphere; it is extending from the sea surface up to heights of 8 to 10 km at polar, 10 to 12 km at the moderate latitudes and up to 16 to 18 km at the equator. In the troposphere, the percentage of gas constituents of the atmosphere dose not vary with height, remaining practically the same as it is at the surface. The only component that varies is water vapor content depending strongly on weather conditions [4]. The water vapor contained in the troposphere comes from surface of oceans, seas, wet land and vegetation. One of the main properties of the troposphere is that temperature decreases with height. The average vertical temperature gradient of the troposphere is 6.5K per kilometer of height. Pressure also decreases with height. The average pressure at the earth's surface is 1.014 bar. At an altitude of 5km, it is nearly halved, at 11km it is 225mb, while at an altitude of 17km the atmosphere pressure is 90mb only [5].Refractivity N depends on pressure, temperature and humidity of the air which, in their turn, change with height. The tropospheric scintillation causes fluctuation in the level

of signal when the frequency is more than 10 GHz, together with signal level attenuation by rain, are among the major problems in radio-wave transmission[6]. In particular, scintillation generated on propagation path at low elevation angles often produces considerable signal fading in excess of 10dB. Therefore, a quantitative understanding of the phenomenon is required to design satellite systems operating at low-elevation angles [2].
Under such circumstances many studies on the tropospheric scintillation have been carried out both theoretically and experimentally [7-9], and there have already been proposed several kinds of scintillation prediction methods [10-11]. Among these methods the Tatarskii theory [12] based on atmospheric turbulence theory and the CCIR model [13] based on a one-year measurement can give useful estimates of scintillation fading. Both methods, however, have their own shortcomings in practical application to satellite system design. For example, in the Tatarskii model, finding an appropriate value of a parameter for the fine structure of atmospheric turbulence along a given propagation path is not usually feasible, while the CCIR model does not take into account the meteorological elements which are thought to exercise a major effect. Uysal et.al. [9] derived error performance bounds for coded free-space optical communication systems to mitigate turbulence-induced fading over atmospheric channels. Kramer and Goodman [10] observed the scintillation in the MAGR/S that occurs because the multiple available paths of propagation those are geometrically far apart and rapidly varying.
In this paper, a method would be proposed for studying scintillation occurring on earth space paths with low-elevation angles at satellite communication with frequencies 14/11 GHz. We apply this method in Iraq within standard atmosphere. And it used meteorological elements: *t* (average temperature) and *u* (relative humidity) for Iraq.

2. EXISTING PREDICTION METHODS

Scintillation is rapid variation in signal level, both increases and decreases generally about a relatively constant mean level. Scintillation can result huge fades that occurs at very low elevation angle (<5°) [12]. Scintillation is of two main types, tropospheric scintillation, and ionospheric scintillation as follow:

1- Tropospheric Scintillation: variations induced by small scale refractive effects in lower atmosphere. At C band, tropospheric scintillation increases as the elevation angle (E_L) decrease due to longer path extent [14],
   - E_L >20° small effect, Dissanayake [11] outlined a propagation modeling but for large elevation angle (39°).
   - E_L between 5° - 20° depends on climate.
   - E_L < 5°can be performance-limiting [6].
2- Ionospheric Scintillation: variations induced by ionized particles. The ionospheric scintillation is [6]:
   - Strongly frequency dependent proportional to $1/f^2$.
   - Not dependent on elevation angle.
   - Negligible in Ku band and above.
   - Problem in high sunspot periods in C band.
   - Of limited effects in L band.

Tatarskii [12] introduced a theoretical formulation for the estimate of log-amplitude fluctuations based on the assumption that the spatial structure of the atmospheric refractive index. When the atmospheric turbulence lies in the inertial sub-range where a relation: $R_{min}^2/\lambda \ll l \ll R_{max}^2/\lambda$ is satisfied, Where: R_{min} , R_{max} is the Inner, outer scale of refractive index irregularities; l is the effective path length between the boundary of turbulence and the reception point, λ is the wavelength of the radio wave; the variance σ_x of log-amplitude in dB is given by [12]:

$$\sigma_x = 42.9\left(\frac{2\pi}{\lambda}\right)^{7/6}\int_0^l C_n^2(r)r^{5/6}dr \quad [\mathrm{dB}^2] \tag{1}$$

In this equation, the structure parameter of the refractive index C_n is varying along the earth-space path. It is known that the structure parameter depends not only on the variance of the atmospheric refractive index but also on the outer scale (R_{min}) of irregularities. So, it is not feasible to identify values of such parameters along a given slant path directly from meteorological elements generally available, and as a result it remains difficult to calculate.
For this reason, a more practical model has been presented by the CCIR [13] based on measured data at a frequency of 7.3GHz an elevation angle of 1° and an antenna diameter of 10m with the aid of theoretical scaling for the frequency, elevation angle, and antenna dish diameter. Since the CCIR model is composed of simple factors and is known to yield estimated values close to the measured values reported thus far, it seems to be a good method at present. However, in this method:

1. It may not be appropriate to extrapolate from the result at a 1° elevation angle, which is the most important range when designing satellite communication systems.
2. Parameters representing meteorological elements are not included in the equation, therefore regional and seasonal dependence can not be explained.
3. The estimated value merely provides the standard deviation of the fluctuations and does not cover the estimate of signal fading as a function of time percentage.

3. SCINTILLATION PREDICTION MODELS

3.1 Measured Data Constructing the Model

This section presents a summary of the scintillation measurement [15] necessary for constructing the prediction method. The measured data were obtained in the 11/14 GHz low-elevation angle propagation experiment for one year at the Yamaguchi satellite.

(a) Seasonal and Diurnal Dependence

(1) In regions such as Japan where the seasonal variation of the meteorological environment is considerably large, scintillation has marked seasonal dependence.
(2) The average value σ_x for each month shows refractive index *N* due to water vapor in the atmosphere averaged over one month.
The relationship in our case is given by:

$$\sigma_{x\,ref} = 0.15 + 5.2 \times 10^{-3}N \quad [\mathrm{dB}] \tag{2}$$

(3) The probability density function of amplitude variation (in dB) during relatively short periods of time (approximately one hour) shows a Gaussian distribution including fairly large scintillation whose rms fluctuations (σ_x) are up to 1.6dB.
(4) Distribution of the standard deviation itself for long term variations over a month can be closely approximated with a gamma distribution. Likewise, there is not a very large deviation from the gamma distribution for the yearly basis.

This indicates that each of the two parameters essential for the determination of the gamma distribution is in fact directly determined by the other.
Based on the properties just stated (item 3) the following equation can be derived:

$$x(m,P) = m \times \eta(P) \tag{3}$$

where x is the signal level for m mean value of rms fluctuations in dB and P percent of the time such that relation between η and P is as following:

$$\eta(P) = 1.099 \times 10^4 \int_{\eta}^{\infty} \int_{0}^{\infty} u^8 \exp(-v^2/2u^2 - 10u)\, du\, dv \tag{4}$$

The time percentage factor η can be obtained as a function of the time percentage P from numerical calculations.

Fig. (1) shows three kinds of cumulative time distributions of signal level variation obtained form a one month measurement (Solid lines) together with calculated curves using equation (3) (dotted line). As it is clear from the figure, measured and calculated curves where the signal level is enhanced (namely, P of 50 to 99.99 percent) have a fairly good coincidence. While a noticeable discrepancy exists in the signal fade region, particularly for P of less than one percent. This may be due to the asymmetry of signal level variation between fading and enhancement. **Fig. (2)** shows time percentage factor η (namely x normalized by m) for both signal fading and enhancement of the data shown in **fig. (1)**. The best fit curves for both fading and enhancement are depicted by dotted and solid lines, respectively. The solid line in the figure is the same as the one obtained theoretically in equation (3).

(b) Frequency Dependence

The measured frequency dependence of log-amplitude variation for two frequencies at 11 and 14GHz was 0.45th power of the frequency ratio (namely, $f^{0.45}$) when modeling, however, it is necessary to take into account the dependence of the antenna diameter on frequency.

Scintillation dependence on antenna aperture size due to the averaging effect for spatial fluctuations of waves. Therefore, the averaging effect for the 14GHz signal should be more than that for 11GHz signal when the same antenna is used for the two different frequencies. After eliminating the frequency dependence due to the aperture averaging effect, a net frequency dependence of $f^{0.45}$ can be derived in the suggested case [16].

(c) Elevation angle Dependence

During the course of 4 year measurement at Yamaguchi, long term data for elevation angle of 4° (satellite: 57° E), 6.5° (60° E) and 9° (63° E) the power of $\csc\theta$ was about 1.3.

3.2 Proposed Prediction Method

Following the basic formulation technique employed in the CCIR model and, a basic equation can be obtained by [15, 16].

Case 1:

When the elevation angle $\theta \leq 5°$, the magnitude of scintillation σ_x (rms fluctuation) is simply given by:

$$\sigma_x = \sigma_{x\,ref}\eta_f\eta_\theta\eta_{D_a} \quad \text{[dB]} \tag{5}$$

where

$$\eta_f = (f/11.5)^{0.45} \tag{6}$$

$$\eta_\theta = (\csc\theta \,/\, \csc 6.5°)^{1.3} \tag{7}$$

or

$$\eta_\theta = \frac{2h}{\sin\theta + \sqrt{\sin^2\theta + \frac{2h}{R_e}}} \tag{8}$$

where $R_e =$ is effective earth radius (=8500km), h is effective height of water vapor in atmosphere (= 2km in this model). And

$$\eta_{D_a} = \sqrt{Q(R)/Q(7.6)} \tag{9}$$

where the antenna diameter dependent factor $Q(R)$ is given below [7], from a piecewise linear approximation of the antenna aperture averaging factor is given by:

$$\left.\begin{array}{ll} Q(R) = 1.0 - 1.4\left(R/\sqrt{\lambda L}\right) & \text{for } 0.0 \le R/\sqrt{\lambda L} \le 0.5 \\ Q(R) = 0.5 - 0.4\left(R/\sqrt{\lambda L}\right) & \text{for } 0.5 \le R/\sqrt{\lambda L} \le 1.0 \\ Q(R) = 0.1 & \text{for } 1.0 \le R/\sqrt{\lambda L} \end{array}\right\} \tag{10}$$

where:
$R =$ The effective radius of circular antenna aperture (m) given by $R = 0.75(D_a/2)$.
$D_a =$ The diameter of reflector (m).
$\lambda =$ The operating wave length (m).
L=Slant distance to height of a horizontal thin turbulent layer $(= \eta_\theta)$ is given by equation (8).

Case 2:
When the elevation angle is above 5°, the magnitude of scintillation σ_x (rms fluctuation) is given by [16]:

$$\sigma_x = 0.0228\sigma_{x\,ref} f^{0.45} \csc^{1.3}\theta \sqrt{Q(D_a)} \quad \text{[dB]} \tag{11}$$

where: $\sigma_{x\,ref}$ is define in equation (2).
In both cases, N is the refractive index given by:

$$N = 3730ue_s/(t+273)^2 \tag{12}$$

where: t is the average temperature (C°), u is the relative humidity (percent) and e_s is the saturated vapor pressure (mb). In this equation e_s can be approximated as a function of temperature t by the following equation [16]:

$$e_s = 6.11\exp\left(19.7t/(t+273)\right) \tag{13}$$

Furthermore, signal level variation $x(P)$ corresponding to P percent of the cumulative time distribution is given by:

$$x(P) = \eta(P) \times \sigma_x(f, \theta, D_a, t, u) \quad \text{[dB]} \tag{14}$$

where the time percentage factor η can be approximated by:

$$\eta(P) = -0.0597(\log P')^3 - 0.0835(\log P')^2 - 1.258 \log P' + 2.672 \quad (15)$$

for $50 < P < 99.9$ (signal enhancement), where $P' = 100 - P$.
or,

$$\eta(P) = -0.061(\log P)^3 + 0.072(\log P)^2 - 1.71 \log P + 3 \quad (16)$$

for $0.01 < P < 50$ (signal fading).
Equation (15) approximates the solid line while equation (16) represents the dotted line in **fig. (2)**.
The model presented here includes meteorological element t (average temperature) and u (relative humidity). In this model, temperature t and humidity u are values determined by averaging for period of around a month so that the model does not predict the magnitude of short-term scintillation varying with daily changes of weather.

4. RESULTS

Several calculation results using the proposed model are presented in this section, proposed model can gives verity of estimates for scintillation fading, depending on meteorological conditions.
In all cases, the rms magnitude of scintillation would be increased with the increasing of relative humidity, besides it would be increased with increasing of temperature and frequency with each relative humidity; for illustration, **fig. (3)** is drawn using different values of t , u and f (at $\theta = 7°, D = 5$m.)
So, in the following comparisons, we'll consider only the relative humidity of 0.6% just to make the results easier to be illustrated.

4.1 Magnitude of Scintillation at an Elevation Angle of 5^o (Case I)

Fig. (4) represents both the effect of frequency and antenna diameter changes on the magnitude of scintillation (rms fluctuation). This shows the calculated σ_x as function of t at f = 11 and 14 GHz, antenna diameter = 3, 6 and 9 m.
From this figure, we can conclude that the magnitude of scintillation (rms fluctuation) would be:

1. Increased with the increasing of the frequency at the same antenna diameter.
2. Decreased with increasing of antenna diameters at the same frequency.

4.2 Magnitude of Scintillation when an Elevation Angle Above 5^o (Case II)

Fig. (5) shows the calculated rms fluctuation due to the scintillation as function of temperature when f = 12GHz at the elevation angle $\theta = (6°, 8°, 12°$ and $20°)$ and antenna diameter D = 3, 6 and 9 m. This figure is telling us that at a certain frequency value, the magnitude of scintillation (rms fluctuation) would be:

1. Obviously decreased with increasing of elevation angle.
2. Decreased with increasing of antenna diameters, differences become smaller when θ get larger.

The calculated rms fluctuation due to the scintillation as function of temperature when f = 11 and 14 GHz and antenna diameter D = 3, 6 and 9 m is shown in **fig. (6)** and **fig. (7)** when the elevation angle $\theta = 7°$ and $12°$ respectively. From these figures, it's clear that the magnitude of scintillation (rms fluctuation) would be:

1. Decreased with increasing of antenna diameters.
2. Increased with the increasing of frequencies.

These properties are similar to the case of 5^{o} elevation angle, and the behavior described in these figures are seemed an extent from **fig. (4)**. When θ become larger, the curves become interfered but σ_x becomes smaller.
The calculated σ_x as function of temperature when when f = 11 and 14 GHz and the elevation angle $\theta = (6°, 8°, 12° \text{ and } 20°)$ with antenna diameter D = 6m is shown in **fig. (8)**.

5. CONCLUSIONS

In this paper, we presented a method of predicting scintillation fading occurring within atmospheric paths with low elevation angles at frequencies 11/14 GHz for standard atmosphere, this method can be applied to worldwide regions with different meteorological conditions. According to the value of the elevation angle, we get the results from the associated case method($\theta \geq 5°$), we found that the amount of scintillation is:

1. *Humidity dependent*: as it increases with the increasing of humidity.
2. *Temperature dependent*: as it would increases with the increasing of temperature.
3. *Frequency dependent*: as it increases with increasing of frequencies 11/14 GHz.
4. *Antenna diameter dependent*: as it decreases with the increasing of antenna diameter.
5. *Elevation angle dependent*: as it decreases with the increasing of elevation angles.

But, generally, for the three variables: (a low elevation angle 5˚-10˚, an operating frequency within the band 11/14GHz and a diameter of the antenna), if we hold two of them at certain values and test for the third, we noticed that the greater impact on the magnitude of scintillation is the elevation angle, the frequency comes secondly while the diameter of the antenna has lowly control.

6. REFERENCES

[1] Rappaport, T. S., "Wireless Communications," 2nd ed., New York: Prentice Hall, 2002.

[2] Seybold, J. S., "Introduction to RF propagation," John Wiley and Sons, Inc. 2005.

[3] Horak, R., "Telecommunications and data communications handbook," John Wiley and Sons, Inc. 2007.

[4] Hu, S., "Modeling the Effects of Ionospheric Scintillation on Satellite to Earth Links", Networks Security, Wireless Communications and Trusted Computing, on Volume 1, April 2009.

[5] Mojoli, L.F.; Mengal, U., "Propagation in Line-of-Sight Radio Link," Publisher by Telettraspa, Milano, Italy, 2001.

[6] Beniguel, Y.; Adam, J.-P.; Noack, T.; Jakowski, N.; Sardon, E.; Valette, J.-J.; Bourdillon, A.; Lassudrie-Duchesne, P.; Arbesser-Rastburg, B., "Signal scintillations in the low latitudes and high latitudes regions", Antennas and Propagation, 2006. First European Conference, Nov. 2006.

[7] Uysal, M.; Li, J.; Yu, M., "Error Rate Performance Analysis of Coded Free-Space Optical Links over Gamma-Gamma Atmospheric Turbulence Channels," IEEE Transactions on Wireless Communications, Vol. 5, No. 6, June 2006.

[8] Yoshio, K.; Yamada, M., "Tropospheric Scintillation in 11/14 GHz Bands on Earth-Space Paths with Low Elevation Angles," IEEE Trans. Antenna Propagation, vol.36, no.4 PP. 563-569, 1988.

[9] Moulsley, T.J. ; E.Vilar., "Experimental and Theoretical States of Microwave Amplitude Scintillation on Satellite Down-Links" IEEE Tran. Antenna Propagation, Vol. AP.30, no.6, PP.1099-1106, 1982.

[10] Dissanayake, A., "Ka-Band Propagation Modeling for Fixed Satellite Applications," Journal of Space Communication Issue No. 2, Fall 2002.

[11] Tatarskii, V. I., "Wave Propagation in a Turbulent Medium" New York, 1961.

[12] Strangeways, H.J.; Gherm, V.E.; Zernov, N.N., "Modeling and mitigation of the effect of scintillations on GPS", ELMAR 2007 Volume , Sept. 2007.

[13] CCIR, "Effects of Tropospheric Refraction on Radio-Wave Propagation" CCIR SG-5. Rep. 718-2, ITU, Geneva, 1986.

[14] Beniguel, Y.; Adam, J.-P.; Prieto-Cerdeira, R.; Arbesser-Rastburg, B., "Ionospheric scintillations at L & C bands". Antennas and Propagation, 2009. 3rd European Conference, March 2009.

[15] Kramer, L.; Goodman, J. L., "Global Scale Observations of Ionospheric Instabilities from GPS in Low Earth Orbit," American Institute of Aeronautics and Astronautics, Inc., 2001.

[16] Yoshio, K., "A New Prediction Method for Tropospheric Scintillation on Earth-Space Paths," IEEE Vol. 36. No.11. P.1608-1614, November 1988.

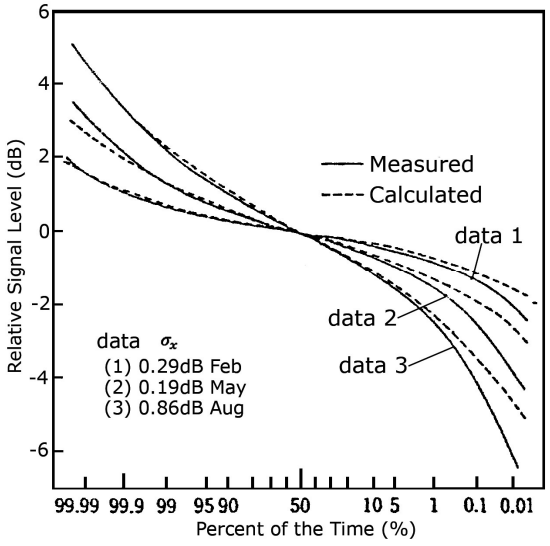

Fig. (1): Cumulative time distribution of long term signal level variation due scintillation [8].

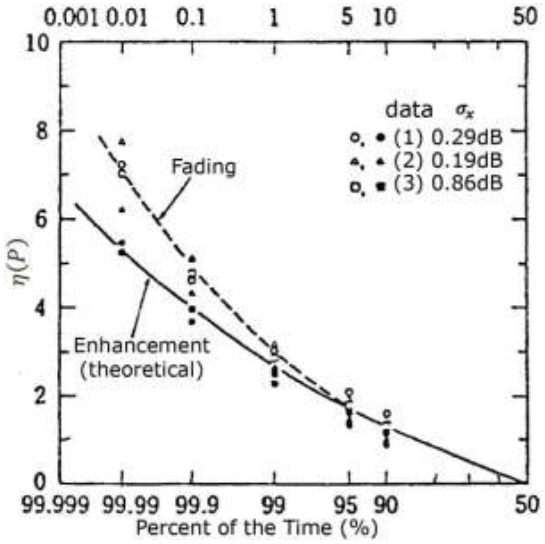

Fig. (2): η factor versus time percentage p [8].

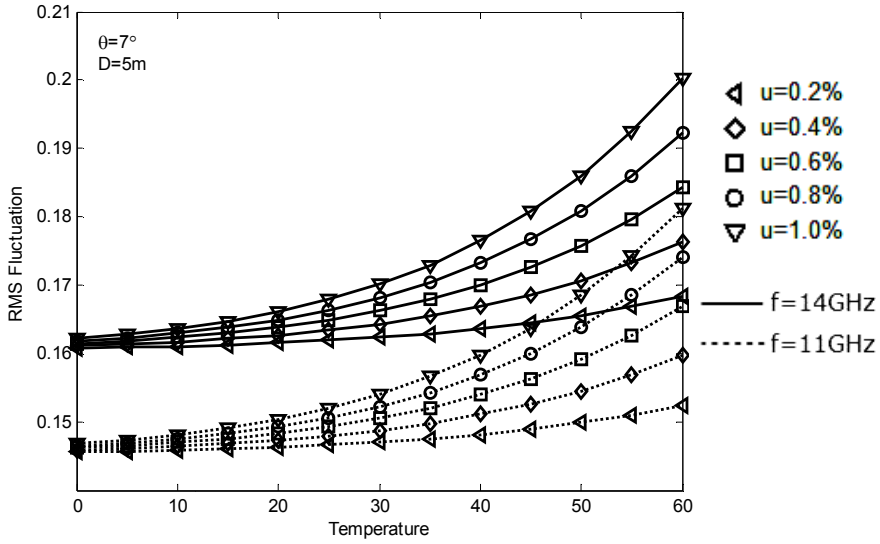

Fig. (3): Relationship between temperature and rms fluctuation at a given u and f.

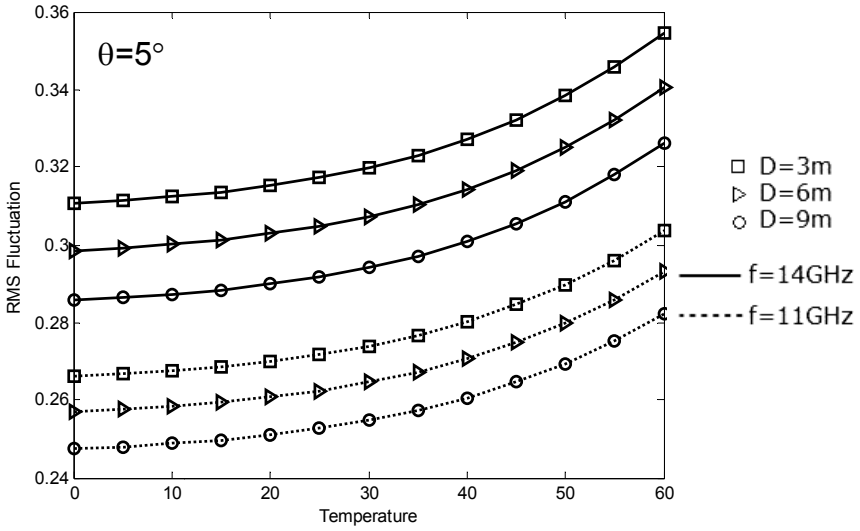

Fig. (4): σ_x versus temperature at different frequencies and antenna diameters.

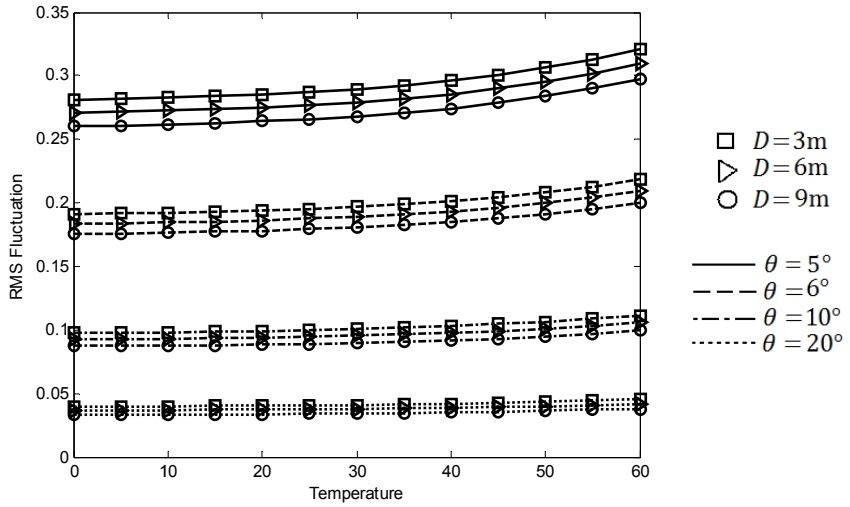

Fig. (5): σ_x versus temperature at different elevation angles and antenna diameters.

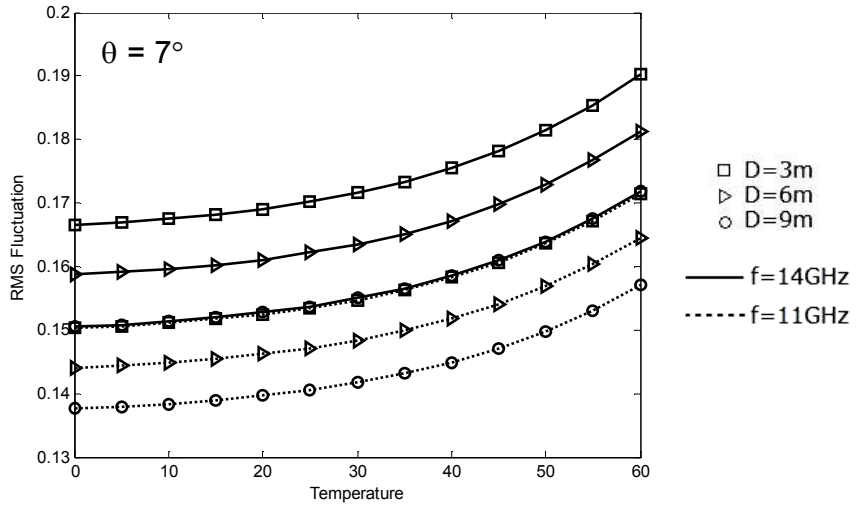

Fig. (6): σ_x versus temperature at different frequencies and antenna diameters at $\theta = 7°$.

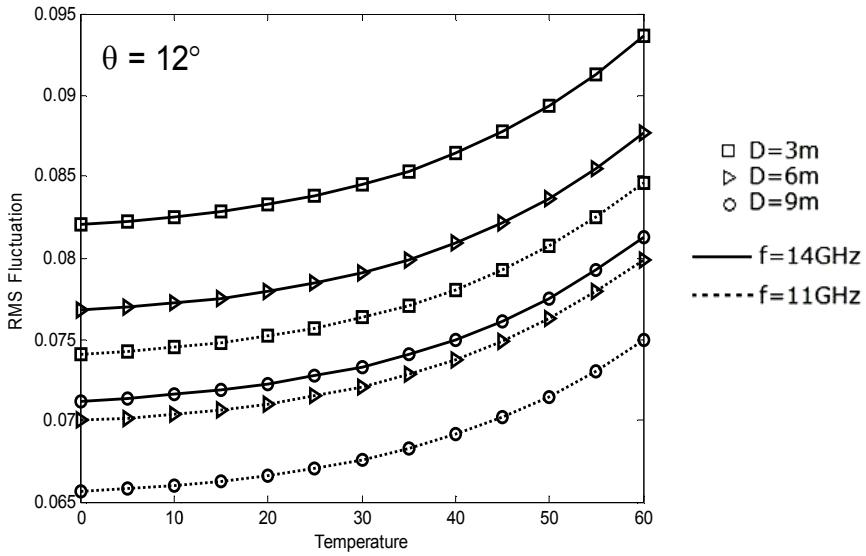

Fig. (7): σ_x versus temperature at different frequencies and antenna diameters at $\theta = 12°$.

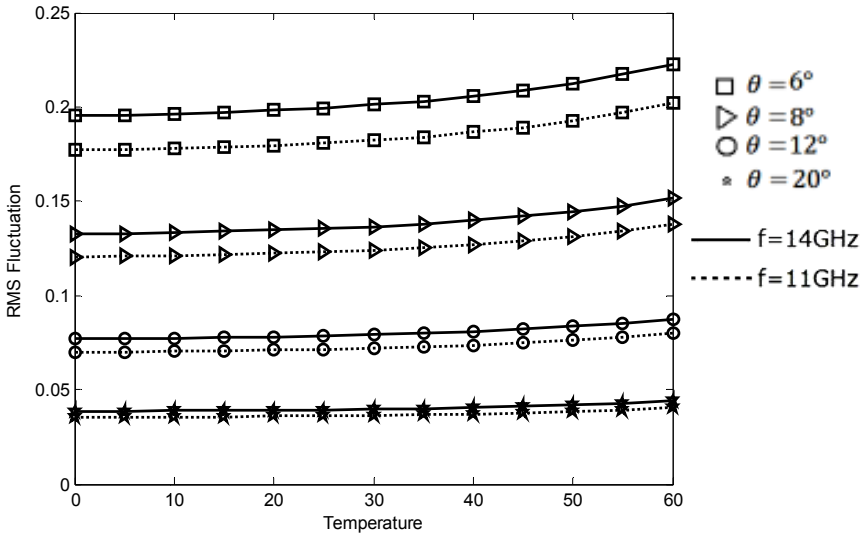

Fig. (8): σ_x versus temperature at different frequencies and elevation angles at D = 6m.

تأثير التألق على إتصالاتِ القمر الصناعي ضمن جوٍّ قياسيٍ

محمد علي حسين
قسم الهندسة الكهربائية، كلية الهندسة
جامعة الانبار، العراق
هاتف: 009647901573394
elecom1978@yahoo.com

الخلاصة:

انتشار الموجات الراديوية خلال الجو يقسم إلى صنفين قياسي وغير قياسي. المشاكل الرئيسة في انتشار الموجات في اتصالات الأقمار الصناعية بالترددات فوق ١٠ كيكا هرتز هي توهين مستوى الإشارة المسبب بواسطة التألق التروبوسفيري بالأضافه إلى توهين مستوى الإشارة بواسطة المطر.

تم اقتراح طريقه منتخبه لقياس التألق في طبقة التروبوسفيري على طريق فضاء الأرض. ولقد تجاوزت هذه الطريقة اغلب المشاكل الموجودة في الطرائق الأخرى المشابهة.

لقد اعتبرنا معدلات قيم الرطوبه و درجه الحراره في معادلات هذه الطريقة حسب اجواء العراق في حالة الجو القياسي وقمنا بدراسة تأثير العناصر الرصديه والتردد وقطر الهوائي وزاوية الارتفاع على مقدار التألق.